Cisplatin Depletes TREX2 and Causes Robertsonian Translocations as Seen in TREX2 Knockout Cells

Ming-Jiu Chen,[1] Lavinia C. Dumitrache,[1] Danny Wangsa,[2] Sheng-Mei Ma,[1] Hesed Padilla-Nash,[2] Thomas Ried,[2] and Paul Hasty[1]

[1]Department of Molecular Medicine/Institute of Biotechnology, The University of Texas Health Science Center at San Antonio, San Antonio, Texas and [2]Genetics Branch, Center for Cancer Research, National Cancer Institute, NIH, Bethesda, Maryland

Abstract

Cisplatin, an anticancer drug, forms DNA interstrand cross-links (ICL) that interfere with replication, whereas TREX2 is a $3' \rightarrow 5'$ exonuclease that removes $3'$ mismatched nucleotides and promotes cellular proliferation. Here, we show that TREX2 is depleted in human cells derived from cancer after exposure to cisplatin but not other genotoxins including another cross-linking agent, mitomycin C (MMC), indicating a potential role for TREX2 depletion in cisplatin-induced cytotoxicity. To better understand TREX2 cellular function, we deleted TREX2 in mouse embryonic stem (ES) cells by gene targeting and find these cells exhibit reduced proliferation and gross chromosomal rearrangements including Robertsonian translocations (RbT). Quite interestingly, ES cells exposed to cisplatin also exhibit RbTs. By contrast, RbTs are not observed for ES cells exposed to MMC, indicating that RbTs are not caused by ICLs but instead TREX2 depletion by either cisplatin exposure or mutation. Taken together, our results show that cisplatin depletes TREX2 and causes genomic instability that is similarly observed in TREX2-mutant cells. Thus, cisplatin has two potential cytotoxic activities: (*a*) the generation of ICLs and (*b*) the depletion of TREX2. [Cancer Res 2007;67(19):9077–83]

Introduction

Platinum-based anticancer drugs, such as cisplatin, generate a variety of DNA lesions including monoadducts, intrastrand cross-links, and interstrand cross-links (ICLs; ref. 1). These ICLs covalently join both DNA strands to disrupt normal metabolic functions that require strand separation like DNA replication and transcription. In addition, a DNA double-strand break (DSB) is formed when the replication fork collides with an ICL (2). Thus, ICLs are extremely cytotoxic, especially for proliferating cells (3).

TREX2 is a $3' \rightarrow 5'$ exonuclease that removes $3'$ mismatched sequences, suggesting that it maintains genomic integrity (4–7). Although the biological significance of TREX2 is largely unknown, this $3' \rightarrow 5'$ exonuclease activity is evolutionarily conserved (8) and present in DNA damage checkpoint proteins (hRad1 and hRad9; refs. 9, 10), DNA repair proteins (MRE11, WRN, APE1, APE2, XPF/ERCC1, and Dna2; refs. 11–16), DNA replication polymerases (polδ, polγ, and polε; refs. 17–19), and the well-known tumor suppressor p53 (20). Functional studies by gene inactivation in yeast and mouse models have shown that mutation in many of these genes leads to genomic instability (8). Additionally, mutations in some of these genes, such as *MRE11, WRN, XPF, polγ*, and *p53*, cause a variety of pathologies, including cancer and/or age-related disease (21–26). Our recent study also suggests that TREX2 maintains genome integrity because it is ubiquitously expressed in tissues and cancer-derived cell lines, forms nuclear foci, and facilitates cellular proliferation (7).

Here, we show that cisplatin reduces cytosolic TREX2 in human cancer-derived cell lines and induces a phenotype common to TREX2-null mouse embryonic stem (ES) cells. After exposure to cisplatin, nuclear TREX2 foci disappear. Subsequently, total cytosolic TREX2 levels are reduced. Wild-type (WT) ES cells exposed to cisplatin, but not mitomycin C (MMC), exhibit Robertsonian translocations (RbT), a phenotype characteristic to TREX2-null ES cells. Thus, ICLs do not ordinarily cause RbTs, supporting the possibility that cisplatin induces a TREX2-null phenotype. Therefore, either cisplatin depletion or genetic deletion of TREX2 causes the same cellular phenotype, suggesting that TREX2 depletion may be responsible for cisplatin-induced cytotoxicity along with ICLs.

Materials and Methods

Cell culture, DNA damage treatment, immunoblotting, and immunostaining for a variety of genotoxins. HeLa cells [American Type Culture Collection (ATCC)] were cultured according to ATCC's instructions. For DNA damage treatment, HeLa cells were seeded at 50% confluency. Next day, DNA-damaging agents were added for 4 h. DNA-damaging agents include streptonigrin (10 nmol/L), paraquat (100 μmol/L), *N*-acetyl-L-cysteine (NAC; 10 mmol/L), methyl methane sulfonate (MMS; 400 μmol/L), *N*-ethyl-*N*-nitrosourea (ENU; 7 mmol/L), cisplatin (0.5 mmol/L), MMC (3 μmol/L), camptothecin (2.5 μmol/L), ICRF-193 (2.25 μmol/L), hydroxyurea (250 μmol/L), aphidicolin (1 μmol/L), 6-thioguanine (10 nmol/L), and trichostatin A (TSA; 1 μmol/L). After 4 h of exposure, cells were collected and lysed in ice-cold lysis buffer [50 mmol/L Tris-HCl (pH 7.5), 1 mmol/L EDTA (pH 8.0), 120 mmol/L NaCl, 0.5% NP40] plus appropriate amount of protease inhibitor cocktails (Sigma). Cell lysates containing 20 to 50 μg of protein were subjected to 10% or 12% SDS-PAGE followed by electrotransfer of resolved protein to nylon membrane. After blocking with nonfat milk (5%) in TBST buffer [Tris-HCl (pH 7.5), 100 mmol/L NaCl, 0.1% Tween 20], the membrane was incubated with the corresponding primary and secondary antibodies (7). The immune complex on the membrane was detected using an enhanced chemiluminescence (ECL) kit (Amersham Pharmacia Biotech).

For immunostaining, HeLa cells were seeded at about 20% to 30% confluence on the chamber slides (Nalge Nunc International Corp.). After 48 h, cells were rinsed with PBS once and then fixed with 4% paraformaldehyde (dissolved in PBS) by incubating at room temperature for 10 min. After three washes with PBS, cells were permeabilized with 0.3%
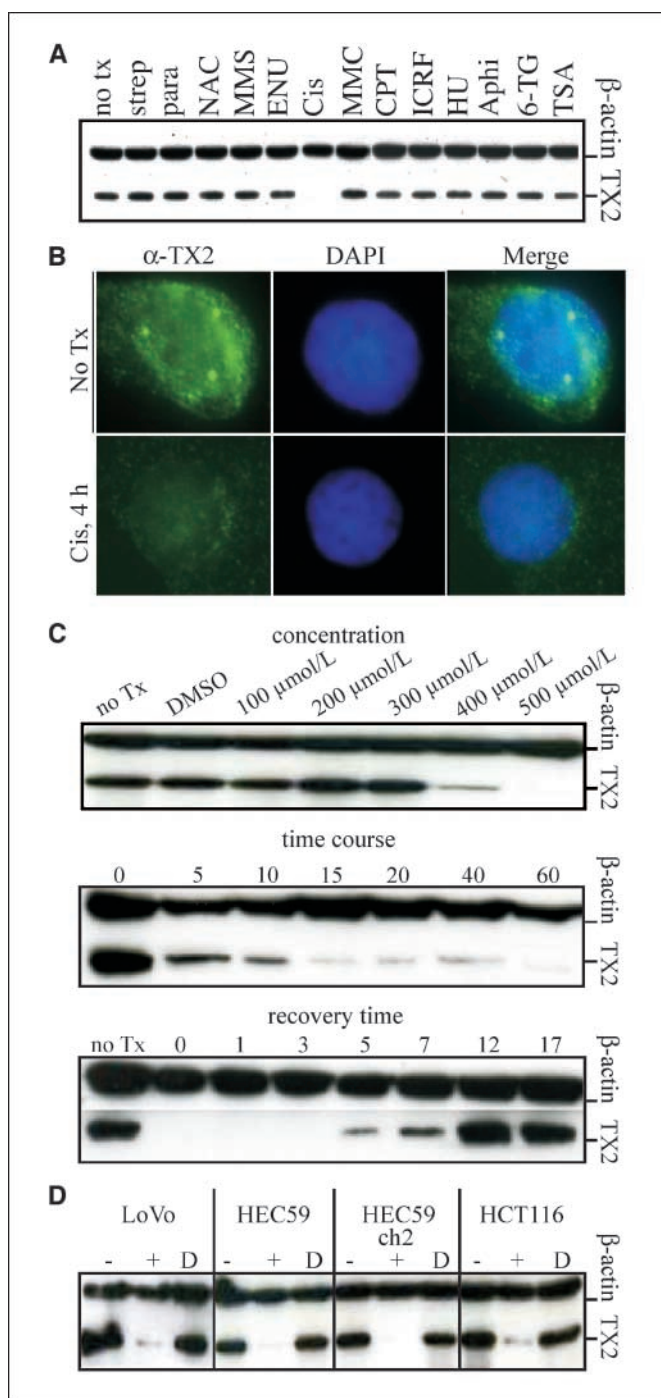
Figure 1. Cisplatin depletes endogenous TREX2 in human cancer-derived cell lines. *A,* endogenous TREX2 protein levels in response to genotoxic agents in HeLa cells. Agents tested are streptonigrin (*strep*; 10 nmol/L), paraquat (*para*; 100 μmol/L), NAC (10 mmol/L), MMS (400 μmol/L), ENU (7 mmol/L), cisplatin (*Cis*; 500 μmol/L), MMC (3 μmol/L), camptothecin (*CPT*; 2.5 μmol/L), ICRF-193 (*ICRF*; 2.25 μmol/L), hydroxyurea (*HU*; 250 μmol/L), aphidicolin (*Aphi*; 1 μmol/L), 6-thioguanine (*6-TG*; 10 nmol/L), and TSA (1 μmol/L). *B,* endogenous TREX2 subcellular localization after exposure to 500 μmol/L cisplatin for either 0 or 4 h in HeLa cells. *C,* dynamics of TREX2 depletion in HeLa cells. *Top,* dose response, 4-h exposure to 100 to 500 μmol/L cisplatin. For zero-dose controls, cells either receive no treatment (*no Tx*) or are exposed to the solvent DMSO at the same concentration as the 500 μmol/L dose. *Middle,* time course in minutes. *Bottom,* pulse chase in hours. Cells are exposed to 500 μmol/L cisplatin for 1 h and then chased for 0 to 17 h. The zero time point is just before removal of cisplatin. *D,* cisplatin depletes TREX2 in a variety of human cancer-derived cell lines. No treatment (−); 4 h of 500 μmol/L cisplatin (+); DMSO (*D*). *ch2,* chromosome 2.

Triton X-100 in TBST for 10 min at room temperature. Following permeabilization, the cells were blocked with the blocking buffer (5% nonfat milk in TBST) for 1 to 2 h at room temperature, and primary antibody (mouse anti-serum, 1:1,000 dilution) was subsequently incorporated to continue incubation for 1 h at room temperature. On the completion of primary antibody incubation, the cells were washed thrice with TBST and then incubated with blocking buffer containing a fluorescent-labeled secondary antibody [working dilution, 1:5,000; Alexa Fluor 488 F(ab')$_2$ fragment of goat anti-mouse IgG (H+L), Molecular Probes] for 1 h at room temperature. After rinse with TBST for three to four times, one drop of 4',6-diamidino-2-phenylindole (DAPI)–containing mounting medium (Vectashield mounting medium, Vector Laboratories, Inc.) was added to the culture slide, and a coverslip was placed on top of the mounting medium. The cells were immediately observed under a Zeiss fluorescent microscope.

Dose response, time course, and pulse chase. Dose response: HeLa cells were seeded at 50% confluency. Next day, 100, 200, 300, 400, and 500 μmol/L of cisplatin and DMSO (corresponding to highest dose of cisplatin) were added for 4 h. Time course: HeLa cells were seeded at 50% confluency and next day, 500 μmol/L cisplatin was added for 5, 10, 15, 20, 40, and 60 min. Pulse chase: HeLa cells were seeded at 50% confluency and next day, 500 μmol/L cisplatin was added for 1 h. Then, cells were washed twice in PBS and then new medium was added for 0, 1, 3, 5, 7, 12, and 17 h.

After cisplatin exposure for any of these experiments, cells were collected and lysed in ice-cold lysis buffer [50 mmol/L Tris-HCl (pH 7.5), 2 mmol/L EDTA (pH 8.0), 150 mmol/L NaCl, 0.5% NP40, 10% glycerol] plus appropriate amount of protease inhibitor cocktails. Cell lysates containing 20 to 50 (25) μg of protein were subjected to 12% SDS-PAGE followed by electrotransfer of resolved protein to nylon membrane. After blocking with nonfat milk (5%) in TBST buffer [Tris-HCl (pH 7.5), 100 mmol/L NaCl, 0.1% Tween 20], the membrane was incubated with the corresponding primary and secondary antibodies. The immune complex on the membrane was detected using an ECL kit.

Analysis of human cancer-derived cells. HEC59 and HEC59+chromosome 2 [a gift from Dr. Thomas Kunkel (National Institute of Environmental Health Sciences, Research Triangle Park, NC)] were cultured as described (27). HeLa (ATCC), HCT116 (ATCC), and LoVo cells (ATCC) were cultured according to ATCC's instructions. Cells were seeded at 50% confluency. Next day, 500 μmol/L cisplatin or DMSO (solvent) was added for 4 h. Immunoblotting was done as described for the dose response, time course, and pulse chase in HeLa cells.

Generation of targeting vector. The TREX2 targeting vector was constructed by amplifying left (5') and right (3') arms using genomic DNA extracted from AB2.2 ES cells (derived from a 129S6/SvEv mouse) by high-fidelity PCR using iProof DNA polymerase (Bio-Rad Laboratories). Reactions were done in 20 μL reaction volume containing 4 μL of 5× iProof HF buffer, 0.4 μL of 10 mmol/L deoxynucleotide triphosphates, 0.25 μL of 4 μmol/L forward or reverse primers (below), 100 ng of genomic DNA, and 0.4 μL of iProof DNA polymerase. The gradient PCR condition is set as follows: 1 cycle of 98°C for 5 min; 30 cycles of 98°C for 1 min → 64.5°C for 1 min with 15°C gradient → 72°C for 1 to 3 min; and 1 cycle of 72°C for 10 min. After amplification, the left arm was cut with *Sal*1 and *Not*1 and cloned into a plasmid backbone cut with *Xho*1 and *Not*1. Then, the right arm was cut with *Xho*1 and *Not*1 and cloned into the same backbone adjacent to the left arm. The entire known mouse *TREX2* coding sequence is deleted. Then, the floxed *HPRT* minigene was cloned into unique Sfi1 sites as described previously (28). The left (5') arm primers were the following: 5'-AAAACGCGTCGACAAGGGAGAGAT-TAATAGGTGTGGAAGGGAGATAGCAAACAGG-3' (mTrxLR5) and 5'-AAAAG-GAAAAGCGGCCGCGGCCACTAAGGCCACAATGAGGCCTAGAGCTGCCA-GAACAAGTGGCATAAGC-3' (mTrxLR31). The right (3') arm primers were the following: 5'-AAAAGGAAAAGCGGCCGCGGCCTGCGTGGCCTA-CAGCCTTCTCTGTACTCCACTATCAGTTGGGCACCTTC-3' (mTrxRR51) and 5'-TACTTTTAAACTCGAGCTGAGCAAGTCAATATACATTTGTAACCCTAG-TACTG-3' (mTrxRR31).

Generation and detection of targeted clones. AB2.2 ES cells were maintained in M15 [[high-glucose DMEM supplemented with 15% fetal bovine serum, 100 μmol/L β-mercaptoethanol, 1 mmol/L glutathione, 3 mg/mL

penicillin, 5 mg/mL streptomycin, and 1,000 units/mL ESGRO [leukemia inhibitory factor (LIF)]] and grown on plates with 2.5×10^6 γ-irradiated murine embryonic fibroblasts (mitotically inactive feeders) seeded on 0.1% gelatin-coated plastic at least the day before and grown in 5% CO_2 in a 37°C incubator at atmospheric O_2. About 10 μg *Pac*I-linearized DNA was mixed with 5×10^6 AB2.2 ES cells in 800 μL PBS. DNA:ES cell mixture was transferred to an electroporation cuvette (Gene Pulser cuvettes, 0.4 cm electrode gap, 10; Bio-Rad Laboratories) and then electroporated at 230 V and 500 μF (Gene Pulser apparatus, Bio-Rad). After electroporation, cells were seeded onto two 10-cm plates with feeders. Next day, M15 medium containing 1× hypoxanthine-aminopterin-thymidine (HAT; 0.1 mmol/L hypoxanthine, 0.0004 mmol/L aminopterin, and 0.016 mmol/L thymidine) was added. After 5 to 7 days of HAT selection, resistant colonies were picked onto a 96-well plate and maintained in HAT selection. After 5 days, these cells were replicated onto gelatin-coated plates. Cells were frozen back on one plate and allowed to proliferate on the other plate for about 5 days. This plate was used to isolate genomic DNA using the microextraction procedure (29). Targeted ES cell clones were screened by genomic PCR for correct gene targeting. Primers to detect left arm integration were TX2 LR55 (outside of left arm) 5′-TATATTTAGGAGACAAAGTGGCCCTGCCAGAGCTG-3′ and HATrev (in the *HPRT* minigene) 5′-CATGCGCTTTAGCAGCCCCGCTGGG-CACTTGGCGC-3′, under the following conditions: 1 round of 98°C for 5 min followed by 35 rounds of 98°C for 1 min, 72°C for 1 min, and 72°C for 2 min and 30 s followed by 1 round of 72°C for 10 min. Primers to detect right arm integration were HATfor (in the *HPRT* minigene) 5′-GTAAAT-GAAAAAATTCTCTTAAACCACAGCACTATTGAG-3′ and TX2 RR33 (outside the right arm) 5′-CCTGTTTCACAAATATCAGGACCTGAGTTTGTATCC-3′, under the following conditions: 1 round of 98°C for 5 min followed by 35 rounds of 98°C for 1 min, 63.5°C for 1 min, and 72°C for 2 min and 30 s followed by 1 round of 72°C for 10 min. Primers to confirm deletion of TREX2 open reading frame (ORF) were 5′-AAAAGAATTCCCGCCACCATGTCT-GAGCCACCCCGGGC-3′ (mTX2For) and 5′-AAAACTCGAGTCAGGCTTC-GAGGCTTGGACC-3′ (mTX2Rev), under the following conditions: 1 round of 98°C for 5 min followed by 35 rounds of 98°C for 1 min, 65°C for 1 min, and 72°C for 25 s followed by 1 round of 72°C for 10 min. Ku80 primers used to control for loading of genomic DNA were 5′-GAGAGTCTACGA-CAACTGTGC-3′ (forward) and 5′-AGAGGGACTGCAGCCATATTA-3′ (reverse), under the following conditions: 1 round of 98°C for 5 min followed by 35 rounds of 98°C for 1 min, 59°C for 1 min, and 72°C for 30 s followed by 1 round of 72°C for 10 min. *Rad51* primers used to control for loading of

cDNA were 5′-CACACCATGGCTATGCAAATGCAGCTTG-3′ (mRAD51For) and 5′-CACACTCGAGTCAAGAGTCATAGATTTTGCAGATTC-3′ (mRA-D51Rev), under the following conditions: 1 round of 98°C for 5 min followed by 35 rounds of 98°C for 1 min, 65°C for 1 min, and 72°C for 40 s followed by 1 round of 72°C for 10 min.

Delete the 5′ half of the *HPRT* minigene. This procedure was done as described previously (28). Briefly, targeted ES cells were grown without HAT for 4 days and then 5×10^6 cells were electroporated with 20 μg Cre expression vector in a total of 800 μL and 200 μL of the electroporation were plated onto a 10-cm feeder plate. Again, cells were grown for 4 days in the absence of selection. After 4 days, cells were trypsinized and 2×10^4 cells were plated onto a 10-cm plate with 6-thioguanine (6-TG) selection medium (10 μmol/L). 6-TG-resistant colonies were picked 10 to 14 days later and expanded for PCR analysis using primers Cre1 and Cre2:
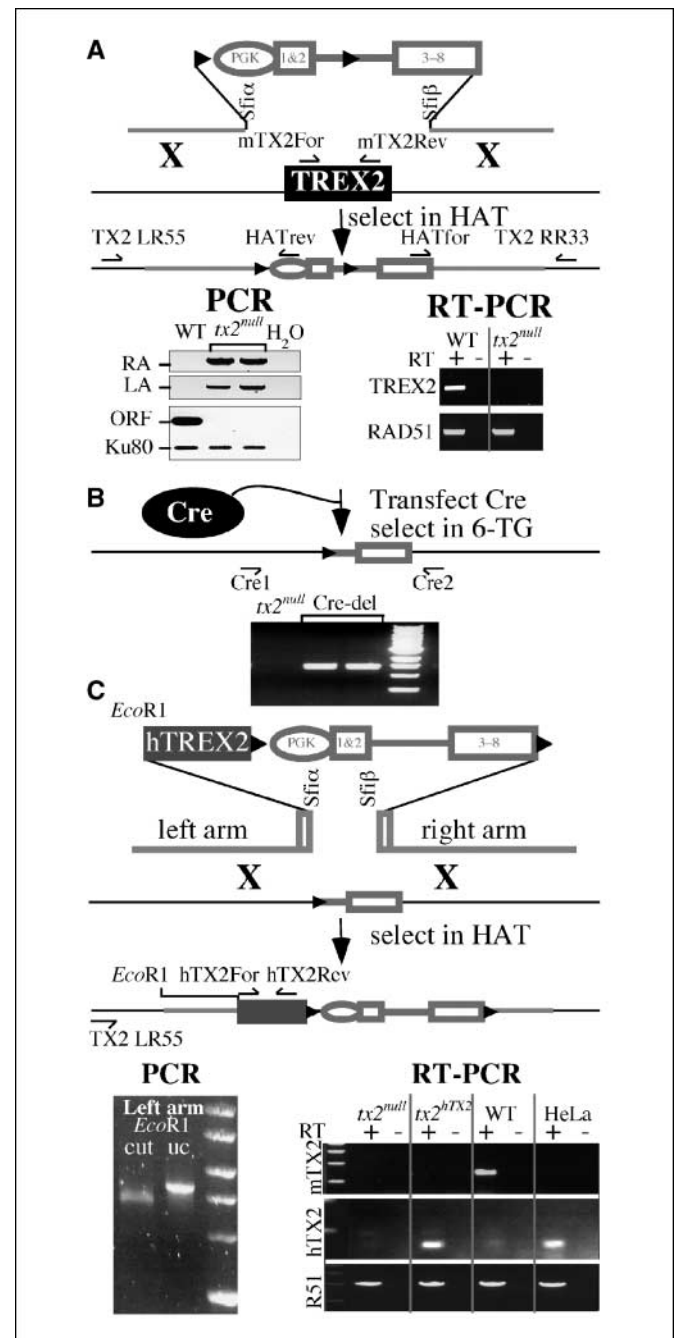

Figure 2. Targeting TREX2 in mouse ES cells. The *HPRT* minigene, expressed by the phosphoglycerate kinase (*PGK*) promoter (34, 41), is used for selection and contains exons 1 and 2 (*box labeled 1 & 2*) and exons 3 to 8 + polyadenylation sequences (*box labeled 3–8*) separated by an intron (*straight line*). Select for minigene expression in HAT. A RE mutant *loxP* (*arrowhead*; ref. 42) is 5′ to phosphoglycerol kinase and another RE mutant *loxP* is in the intron. Sfi1 sites (GGCCNNNNNGGCC) flank this cassette that permit sticky directional cloning because this site generates noncomplementary overhangs. We consistently use two *Sfi*1 sites called *Sfi*α (GGCCTTAGTGGCC) and *Sfi*β (GGCCTGCGTGGCC); thus, selection cassettes can be readily replaced (important for knock-in). *A*, deleting the entire known mouse TREX2 ORF (*black rectangle*); this sequence corresponds to the human short isoform (7). Transfected cells are selected in HAT and targeted clones are screened by PCR (described in Materials and Methods). Two *trex2^null* (*tx2^null*) clones (2E1 and 2F7) are shown. Integration of the left arm (*LA*) is detected with TX2 LR55 and HATrev primers and integration of the right arm (*RA*) is detected with HATfor and TX2 RR33 primers. The mouse TREX2 coding sequence is detected with mTX2For and mTX2Rev. Ku80 is a control to ensure DNA loading. To verify mouse *TREX2* mRNA is absent, these *trex2^null* (*tx2^null*) clones are further tested by RT-PCR (*right*). *Rad51* is used as a positive control to ensure RNA loading. *B*, removal of the 5′ half of the *HPRT* minigene by Cre-mediated recombination. Transiently transfect a Cre expression vector and select in 6-thioguanine (6-TG). 6-Thioguanine (6-TG)–resistant clones were screen for deletion by PCR using primers Cre1 and Cre2. *C*, introduction of the short isoform of human *TREX2* cDNA (hTREX2; *gray box*; ref. 7) into a clone of *trex2^null* cells (2F7). Knock-in of human *TREX2* is verified by PCR (*left*) using TX2 LR55 and hTX2Rev primers for the left arm and this amplified sequence is confirmed by *Eco*R1 restriction digest [uncut (*uc*)]. Expression of human *TREX2* is confirmed by RT-PCR (*right*) using primers unique to human *TREX2* (hTX2For and hTX2Rev) and mouse *TREX2* cDNA (mTX2For and mTX2 Rev). *Rad51* (*R51*) is used as a loading control. *RT*, reverse transcriptase.

5′-CCATGAGTCCTCTTTAAAGTG-3′ (Cre1) and 5′-CCAAAGGCCTCATGA-GATGG-3′ (Cre2), under the following conditions: 1 round of 98°C for 5 min followed by 35 rounds of 98°C for 1 min, 63.5°C for 1 min, and 72°C for 1 min and 30 s followed by 1 round of 72°C for 10 min.

Generation of knock-in vector. The short isoform of the human TREX2 cDNA (7) was amplified from RNA isolated form HeLa cells and then cloned upstream to SV40 polyadenylation sequences and these sequences were inserted adjacent to the *HPRT* minigene. The amplified product was sequenced after cloning to ensure fidelity. We chose to use the short human isoform because only this isoform is commonly detected in the mouse (7). This cassette was cloned into the *Sfi1* sites of the original targeting vector. The primers used were as follows: 5′-AAAAGAATTCCCGCCACCATGTCC-GAGGCACCCGGGC-3′ (hTREX2For) and 5′-AAAACTCGAGTCAGGCCTC-CAGGCTGGGGTC-3′ (hTREX2Rev).

Generation and detection of knock-in clones. *trex2^{null}* cells (deleted for the 5′ half of the *HPRT* minigene) were transfected with the hTREX2 knock-in vector using the same conditions described for the knockout gene targeting vector. Cells were grown and DNA was isolated as described for the knockout. Knock-in clones were identified by PCR and verified by reverse transcription-PCR (RT-PCR). The primers used in PCR to identify targeted clones were 5′-TATATTTAGGAGACAAAGTGGCCCTGCCA-GAGCTG-3′ (TX2 LR55) and 5′-CCTGCAGCGTCCGCACCACG-3′ (hTX2Rev2), under the following conditions: 1 round of 98°C for 5 min followed by 35 rounds of 98°C for 1 min and 72°C for 3 min 30 s followed by 1 round of 72°C for 10 min. The primers used in RT-PCR for mouse TREX2 were 5′-AAAAGAATTCCCGCCACCATGTCTGAGCCACCCCGGGC-3′ (mTX2For) and 5′-AAAACTCGAGTCAGGCTTCGAGGCTTGGACC-3′ (mTX2Rev), under the following conditions: 1 round of 98°C for 5 min followed by 35 rounds of 98°C for 1 min, 65°C for 1 min, and 72°C for 25 s followed by 1 round of 72°C for 10 min. The primers used for RT-PCR for human TREX2 were 5′-AAAAGAATTCCCGCCACCATGTCCGAGG-CACCCCGGGC-3′ (hTX2For) and 5′-CTGCAGCGTCCGCACCACG-3′ (hTX2Rev), under the following conditions: 1 round of 98°C for 5 min followed by 35 rounds of 98°C for 1 min, 65°C for 1 min, and 72°C for 25 s followed by 1 round of 72°C for 10 min.

Proliferation curve. Cells (1×10^4) were seeded onto the gelatin-coated wells of a 24-well plate. Cells were counted with a hemacytometer.

Three-color fluorescence *in situ* hybridization. Treat cells with 10 mg colcemide for 4 h and then trypsinize cells. Slide preparation: spin cells (800 rpm), 10-min wash cells ×2 in PBS (all PBS washes are pH 7.4 unless otherwise noted). Resuspended pellet in 600 mL of 75 mmol/L KCl, dropwise, flicking tube. Incubate 37°C water bath for 15 min. Add 300 mL methanol/acetic acid (2:1 fixative), dropwise, flicking tube, spin at 3,000 rpm, 30 s. Wash cells in 600 mL 2:1 fixative, dropwise, flicking tube, spin at 3,000 rpm, 30 s; rpt wash. Hybridization: place slides in 70 mmol/L NaOH, 2 min. Wash in PBS (pH 8.5), 10 dips. Incubate 37°C, 15 min in the dark, in 500 μL/slide of
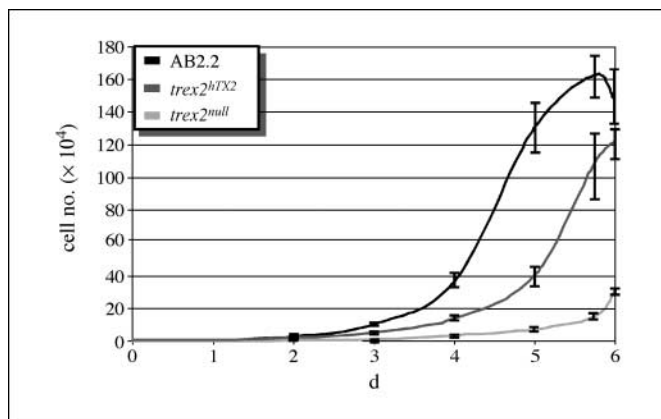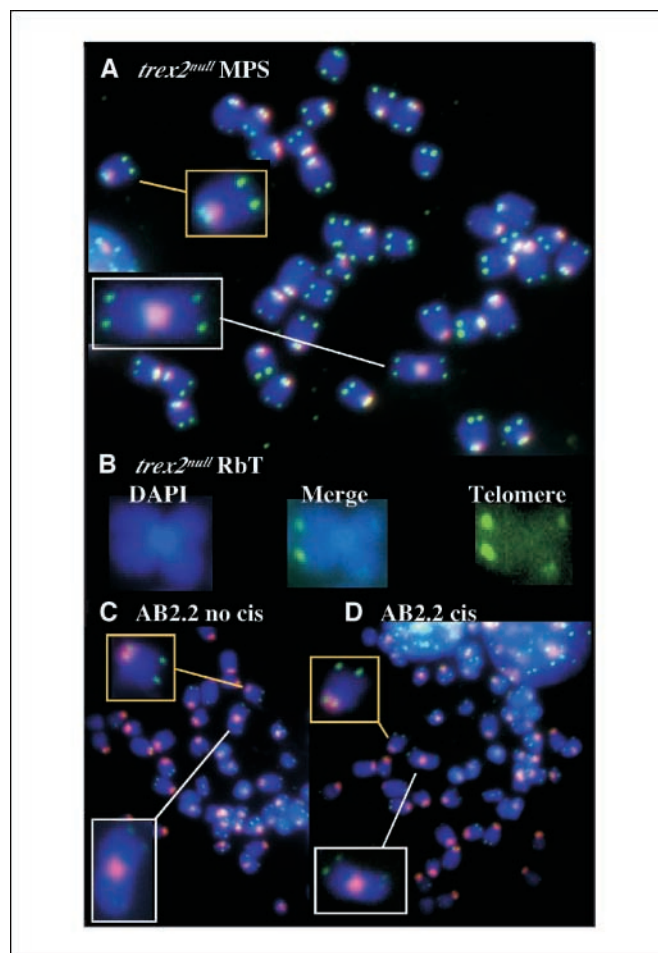

Figure 4. RbTs. Cells were stained with DAPI (*blue*), a MSR probe for the pericentromere (*red*), and a telomere probe (*green*; ref. 35). *White inset*, RbTs; *orange inset*, normal chromosome. *A, trex2^{null}* metaphase spread (MPS) with a RbT. *B,* the RbTs do not contain telomere sequences at the junction. Metaphase spreads stained with DAPI and the telomere probe. The MSR probe was not used because it quenches the signal from potential telomeric sequences at the pericentromere. *C,* the single control (AB2.2) metaphase spread with a RbT from cells not exposed to cisplatin. *D,* control (AB2.2) metaphase spread with a RbT from cells exposure to 250 μmol/L cisplatin for 5 h.

0.25 mg/mL major satellite repeat (MSR; CY-3 5′-TGGAATATGGCGAGAA-AACTGAAAATCATGGAAAATGAGA-3′) and telomere probes [6-FAM 5′-(CCCTAA)$_7$-3′] wash in PBS, 10 dips, coverslip in DAPI.

Spectral karyotyping. Frozen mouse ES cells were resuspended in fresh M15 in LIF. Next, the cells were centrifuged and plated onto gelatin-coated six-well plates. The cells were usually ready to be harvested for metaphase spreads after 48 to 72 h of culture.

Spectral karyotyping (SKY) was done as described earlier (30). For details see, the Web site.[3] Metaphase cell suspensions were dropped onto clean glass slides inside a humidity chamber. Slides were then hybridized with the combinatorially labeled whole chromosome painting probes. After stringent washes with 50% formamide/2× SSC, followed by antibody incubations, metaphase images are captured using the Applied Spectral Imaging spectrophotometer (Applied Spectral Imaging, Inc.) on an epifluorescence microscope. SKY karyotypes were then analyzed with SKY view version 1.62 software (Applied Spectral Imaging). For each SKY case, 10 to 15 metaphases were captured and analyzed using mouse nomenclature rules from The Jackson Laboratory.[4]

Figure 3. Proliferation curve. Control cells (AB2.2; *dark tone*), *trex2^{hTX2}* cells (*middle tone*), and *trex2^{null}* cells (*light tone*).

Results and Discussion

Cisplatin reduces cytosolic TREX2. Human TREX2 levels were measured after exposure to a variety of genotoxic agents in HeLa cells (human cervix adenocarcinoma cells from ATCC) to test if it is important for DNA repair because TREX2 displays properties, suggesting that it plays such a role ($3' \rightarrow 5'$ exonuclease activity, forms nuclear foci and facilitates cellular proliferation; ref. 7). By Western blot, we find that TREX2 is depleted after 4 h of exposure to 500 µmol/L cisplatin, a DNA cross-linking agent (Fig. 1*A*), and by immunofluorescence, we find that TREX2 nuclear foci disappear (Fig. 1*B*). However, under the conditions tested, TREX2 levels remain unchanged after exposure to other genotoxins including another cross-linking agent, MMC. Thus, chemical depletion of TREX2 seems to be unique to cisplatin.

We next measured the dynamics of cisplatin-mediated TREX2 depletion in HeLa cells (Fig. 1*C*). The concentration of cisplatin required to deplete TREX2 was measured after 4 h of exposure. A concentration of 300 µmol/L is insufficient to deplete TREX2, whereas 400 µmol/L cisplatin depletes most TREX2 and 500 µmol/L cisplatin depletes all TREX2 as visualized by Western blot. The time required for 500 µmol/L cisplatin to deplete TREX2 was measured. TREX2 levels diminish after 5 min and are completely gone after 60 min. The time required for TREX2 levels to recover was measured after 1-h exposure to 500 µmol/L cisplatin. After a 1-h pulse, TREX2 levels begin to recover by 5 h and are completely reestablished after 12 h. These results show that a 1-h exposure to 500 µmol/L cisplatin is required to deplete TREX2. In addition, cisplatin-induced TREX2 depletion is reversible after 5 to 12 h. Therefore, physiologically relevant concentrations of cisplatin are sufficient to quickly deplete TREX2 because ∼10% of HeLa cells are viable after 6 days of exposure to 400 µmol/L cisplatin (31).

We next determined if cisplatin depletes TREX2 in other human cancer-derived cells: LoVo (colorectal adenocarcinoma epithelial cells from ATCC), HEC59 (endometrial tumor cells defective for MSH2; ref. 27), HEC59+chromosome 2 (MSH2 complemented; ref. 32), and HCT116 (colon cancer epithelial cells defective for MLH1 from ATCC). Previously, we showed that TREX2 is expressed in most human cancer-derived cell lines, suggesting that it has a common cellular function (7). Similar to HeLa cells, 4-h exposure to 500 µmol/L cisplatin depletes TREX2 for these other cell lines (Fig. 1*D*). Therefore, cisplatin depletion of TREX2 seems to occur in a variety of human cancer-derived cell lines. In addition, loss of mismatch repair proteins like MLH1 can result in resistance to

cisplatin (33); thus, cisplatin reduces TREX2 in cells that are mismatch repair defective and resistant to cisplatin.

Cisplatin is an interstrand DNA cross-linker and ICLs are known to cause DSBs at replication forks (2) that are toxic to proliferating cells. Now, we show that cisplatin effectively reduces cytosolic TREX2; therefore, TREX2 depletion could also contribute to the cytotoxicity of cisplatin assuming that TREX2 is important for cellular viability and genome maintenance. This assumption seems possible because TREX2 has $3' \rightarrow 5'$ exonuclease activity, forms nuclear foci, and facilitates cellular proliferation, suggesting that it is important for chromosomal maintenance (7).

TREX2 facilitates proliferation and suppresses RbTs. The *TREX2* coding sequence was deleted in mouse ES cells (AB2.2) by gene targeting (Fig. 2*A*) to determine if cisplatin-induced TREX2 depletion causes a similar phenotype as genetic TREX2 deletion. A single exon that contains the entire known mouse coding sequence was replaced with the *HPRT* minigene (34); this coding sequence corresponds to the human short isoform (7). *TREX2*-targeted clones are hemizygous null because it is located on the X chromosome and because AB2.2 ES cells are XY. These mutated cells are called *trex2^null* and two mutant clones are analyzed: 2E1 and 2F7.

The short isoform of the human cDNA (7) is targeted back into *trex2^null* cells (clone 2F7) by a two-step process (there is 89.8% identity between these human and mouse proteins). The first step removes the $5'$ half of the *HPRT* minigene by Cre-mediated recombination and selection in 6-thioguanine (Fig. 2*B*; ref. 28). The second step targets the human *TREX2* cDNAs back into these *trex2^null* cells positioning it adjacent to the mouse *TREX2* promoter (Fig. 2*C*). These humanized clones express the short isoform of human TREX2 (7) and are called *Trex2^hTX2* (three clones are analyzed).

TREX2 is likely important for cellular proliferation because, previously, we showed that RNA interference knockdown of TREX2 decreased cellular proliferation in HeLa cells (7). Here, we confirm this observation in mouse ES cells because both *trex2^null* clones exhibit slower proliferation than control cells and because this phenotype is partially rescued by expression of human TREX2 (Fig. 3). Thus, TREX2 depletion impairs cellular proliferation in both mouse ES cells and in human HeLa cells.

We observed metaphase spreads by three-color fluorescence *in situ* hybridization (FISH) to identify gross chromosomal rearrangements (GCR) for control and *trex2^null* cells (Fig. 4; Table 1). These cells were treated with 10 mg colcemide for 4 h and stained with a subtelomere probe (green), a MSR probe in the

Table 1. Summary of three-color FISH and SKY

		Three-color FISH			SKY			
	Agent	MPS (Ab no.)	%1 RbT	%2 RbT	MPS (Ab no.)	%Del	%Trans	%Dup
AB2.2	—	400 (1)	0.25	0	16 (2)	12	0	0
trex2^null	—	140 (22)	15	0.7	29 (13)	34	10	24
trex2^hTX2	—	270 (5)	1.8	0	—	—	—	—
AB2.2	cis	436 (16)	3.4	0.2	—	—	—	—
trex2^null	cis	83 (1)	1.2	0	—	—	—	—
AB2.2	MMC	400 (0)	0	0	—	—	—	—
trex2^null	MMC	200 (6)	3.0	0	—	—	—	—

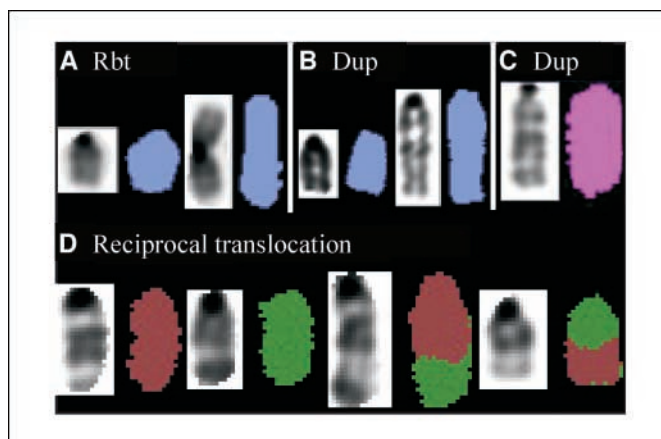Abbreviations: Ab, abnormal; Del, deletions; Trans, translocations; Dup, duplications.

Figure 5. SKY analysis shows GCRs for *trex2^null* metaphase chromosomes. *A,* RbT (11:11). *B,* duplication (*Dup*) of chromosome 11A2. *C,* duplication of chromosome 12. *D,* reciprocal translocation between chromosomes 5 (*brown*) and 10 (*green*).

pericentromere (red), and DAPI (blue; ref. 35). About 0.25% of control metaphase spreads compared with 16% of *trex2^null* metaphase spreads exhibit spontaneous RbTs ($P < 0.0001$, Fisher's exact test on binomial data; Fig. 4*A*; see Supplementary Table S1 for absolute numbers and summary of statistical analysis). RbTs are chromosome rearrangements that involve the centric fusion of two acrocentric chromosomes to form a single metacentric chromosome (36) and are known to increase cancer risk (37), spontaneous abortions (38), and male infertility (39). These RbTs do not contain telomeres at the fusion site as observed by two-color FISH (only DAPI and the telomere probe were used; Fig. 4*B*). RbTs are not due to a single event that was subsequently expanded within the population of cells because they are found in both clones at equal frequency (Supplementary Table S1). Additionally, expression of human TREX2 in *trex2^null* cells significantly decreases RbT levels to ∼1.8% ($P = 0.042$, Fisher's exact test on binomial data; Table 1; Supplementary Table S1).

In addition to three-color FISH, SKY was done to more completely evaluate *trex2^null* cells for GCRs (Fig. 5; Table 1; Supplementary Table S1). In 16 control metaphase spreads, we observed three deletions but no duplications or translocations. In 29 metaphase spreads prepared from *trex2^null* cells, we detected 9 deletions, 7 duplications, and 3 translocations. Thus, there are a total of 3 GCRs for 16 control metaphase spreads compared with 19 GCRs for 29 *trex2^null* metaphase spreads ($P = 0.0463$, Fisher's exact test on binomial data). Excluding deletions, there are no GCRs for 16 control metaphase spreads compared with 10 GCRs for 29 *trex2^null* metaphase spreads ($P = 0.0080$, Fisher's exact test on binomial

data). These GCRs include a RbT (11:11; Fig. 5*A*), a duplication of chromosome 11 (Fig. 5*B*) and chromosome 12 (Fig. 5*C*), and two reciprocal translocations [t(5E; 10C) (10C; 5E) (Fig. 5*D*) and t(12E; 18D) (18D; 12E); data not shown]. Thus, both three-color FISH and SKY identify RbTs and SKY additionally identifies other GCRs that are difficult to observe by three-color FISH. These data show that TREX2 maintains genomic stability by suppressing GCRs and suggest that responses to DNA damage reduce proliferation for *trex2^null* cells as shown in Fig. 3.

Cisplatin, but not MMC, induces RbTs. To determine if cisplatin-induced TREX2 depletion results in a TREX2-null phenotype, WT AB2.2 ES cells were exposed for 5 to 10 h to 250 μmol/L cisplatin or 100 nmol/L MMC and then exposed for 4 h to 10 mg colcemide so that metaphase spreads may be evaluated for RbTs by three-color FISH (Table 1; Supplementary Table S1). We find that RbTs are rare (0.25%) for unexposed AB2.2 cells (Fig. 4*C*). However, RbTs increase by 15-fold (3.7%) after exposure to cisplatin ($P = 0.0003$, Fisher's exact test on binomial data; Fig. 4*D*), but not MMC ($P < 0.0001$, comparing the number of RbTs for AB2.2 cells exposed to either cisplatin or MMC). The total number of RbTs decreases in *trex2^null* cells after exposure to either cisplatin or MMC such that the incidence of RbTs is about the same as WT cells exposed to cisplatin (Table 1; Supplementary Table S1). Previously, cross-linking agents were shown to disrupt RbTs, suggesting that the fusion site is structurally fragile (40); thus, these data suggest that cisplatin-induced TREX2 depletion induces RbTs, whereas both cisplatin and MMC disrupt RbTs such that the total number of RbTs rests in the balance.

Conclusion. We show that TREX2 is depleted after exposure to cisplatin in human cancer-derived cell lines. Cisplatin-induced TREX2 depletion seems to cause a TREX2-null phenotype because cisplatin-exposed cells exhibit RbTs as do cells deleted for TREX2 by gene targeting. In addition, we show that TREX2 is important for efficient cellular proliferation and for maintaining genomic stability by suppressing GCRs. Thus, cisplatin may have two cytotoxic modes of action to inhibit cellular proliferation and induce genomic instability: (*a*) ICL generation and (*b*) TREX2 depletion.

Acknowledgments

References

1. Yang XL, Wang AH. Structural studies of atom-specific anticancer drugs acting on DNA. Pharmacol Ther 1999; 83:181–215.
2. Bessho T. Induction of DNA replication-mediated double strand breaks by psoralen DNA interstrand cross-links. J Biol Chem 2003;278:5250–4.
3. Dronkert ML, Kanaar R. Repair of DNA interstrand cross-links. Mutat Res 2001;486:217–47.
4. Mazur DJ, Perrino FW. Identification and expression of the TREX1 and TREX2 cDNA sequences encoding mammalian 3′→5′ exonucleases. J Biol Chem 1999;274: 19655–60.
5. Mazur DJ, Perrino FW. Structure and expression of the TREX1 and TREX2 3′→5′ exonuclease genes. J Biol Chem 2001;276:14718–27.
6. Mazur DJ, Perrino FW. Excision of 3′ termini by the Trex1 and TREX2 3′→5′ exonucleases. Characterization of the recombinant proteins. J Biol Chem 2001;276: 17022–9.
7. Chen MJ, Ma SM, Dumitrache LC, Hasty P. Biochemical and cellular characteristics of the 3′→5′ exonuclease TREX2. Nucleic Acids Res 2007;35:2682–94.
8. Shevelev IV, Hubscher U. The 3′ 5′ exonucleases. Nat Rev Mol Cell Biol 2002;3:364–76.
9. Parker AE, Van de Weyer I, Laus MC, et al. A human homologue of the Schizosaccharomyces pombe rad1+ checkpoint gene encodes an exonuclease. J Biol Chem 1998;273:18332–9.
10. Bessho T, Sancar A. Human DNA damage checkpoint protein hRAD9 is a 3′ to 5′ exonuclease. J Biol Chem 2000;275:7451–4.
11. Paull TT, Gellert M. The 3′ to 5′ exonuclease activity of Mre 11 facilitates repair of DNA double-strand breaks. Mol Cell 1998;1:969–79.

12. Huang S, Li B, Gray MD, Oshima J, Mian IS, Campisi J. The premature ageing syndrome protein, WRN, is a $3' \rightarrow 5'$ exonuclease [letter]. Nat Genet 1998;20:114–6.

13. Chou KM, Kukhanova M, Cheng YC. A novel action of human apurinic/apyrimidinic endonuclease: excision of L-configuration deoxyribonucleoside analogs from the 3′ termini of DNA. J Biol Chem 2000;275:31009–15.

14. Mu D, Bessho T, Nechev LV, et al. DNA interstrand cross-links induce futile repair synthesis in mammalian cell extracts. Mol Cell Biol 2000;20:2446–54.

15. Burkovics P, Szukacsov V, Unk I, Haracska L. Human Ape2 protein has a 3′-5′ exonuclease activity that acts preferentially on mismatched base pairs. Nucleic Acids Res 2006;34:2508–15.

16. Masuda-Sasa T, Imamura O, Campbell JL. Biochemical analysis of human Dna2. Nucleic Acids Res 2006;34: 1865–75.

17. Chung DW, Zhang JA, Tan CK, Davie EW, So AG, Downey KM. Primary structure of the catalytic subunit of human DNA polymerase δ and chromosomal location of the gene. Proc Natl Acad Sci U S A 1991;88:11197–201.

18. Ropp PA, Copeland WC. Cloning and characterization of the human mitochondrial DNA polymerase, DNA polymerase γ. Genomics 1996;36:449–58.

19. Kesti T, Frantti H, Syvaoja JE. Molecular cloning of the cDNA for the catalytic subunit of human DNA polymerase ε. J Biol Chem 1993;268:10238–45.

20. Mummenbrauer T, Janus F, Muller B, Wiesmuller L, Deppert W, Grosse F. p53 protein exhibits 3′-to-5′ exonuclease activity. Cell 1996;85:1089–99.

21. Carney JP, Maser RS, Olivares H, et al. The hMre11/hRad50 protein complex and Nijmegen breakage syndrome: linkage of double-strand break repair to the cellular DNA damage response. Cell 1998;93:477–86.

22. Stewart GS, Maser RS, Stankovic T, et al. The DNA double-strand break repair gene hMRE11 is mutated in individuals with an ataxia-telangiectasia-like disorder. Cell 1999;99:577–87.

23. Yu CE, Oshima J, Fu YH, et al. Positional cloning of the Werner's syndrome gene. Science 1996;272:258–62.

24. Thompson LH, Brookman KW, Weber CA, et al. Molecular cloning of the human nucleotide-excision-repair gene ERCC4. Proc Natl Acad Sci U S A 1994;91: 6855–9.

25. Van Goethem G, Dermaut B, Lofgren A, Martin JJ, Van Broeckhoven C. Mutation of POLG is associated with progressive external ophthalmoplegia characterized by mtDNA deletions. Nat Genet 2001;28:211–2.

26. Soussi T, Kato S, Levy PP, Ishioka C. Reassessment of the TP53 mutation database in human disease by data mining with a library of TP53 missense mutations. Hum Mutat 2005;25:6–17.

27. Umar A, Koi M, Risinger JI, et al. Correction of hypermutability, N-methyl-N'-nitro-N-nitrosoguanidine resistance, and defective DNA mismatch repair by introducing chromosome 2 into human tumor cells with mutations in MSH2 and MSH6. Cancer Res 1997;57: 3949–55.

28. Holcomb VB, Kim TM, Dumitrache LC, Ma SM, Chen MJ, Hasty P. HPRT minigene generates chimeric transcripts as a by-product of gene targeting. Genesis 2007; 45:275–81.

29. Ramirez-Solis R, Rivera-Perez J, Wallace JD, Wims M, Zheng H, Bradley A. Genomic DNA microextraction: a method to screen numerous samples. Anal Biochem 1992;201:331–5.

30. Schrock E, du Manoir S, Veldman T, et al. Multicolor spectral karyotyping of human chromosomes. Science 1996;273:494–7.

31. Marple T, Li H, Hasty P. A genotoxic screen: rapid analysis of cellular dose-response to a wide range of agents that either damage DNA or alter genome maintenance pathways. Mutat Res 2004;554:253–66.

32. Wu Q, Christensen LA, Legerski RJ, Vasquez KM. Mismatch repair participates in error-free processing of DNA interstrand crosslinks in human cells. EMBO Rep 2005;6:551–7.

33. Aebi S, Kurdi-Haidar B, Gordon R, et al. Loss of DNA mismatch repair in acquired resistance to cisplatin. Cancer Res 1996;56:3087–90.

34. Reid LH, Gregg RG, Smithies O, Koller BH. Regulatory elements in the introns of the human HPRT gene are necessary for its expression in embryonic stem cells. Proc Natl Acad Sci U S A 1990;87:4299–303.

35. Guenatri M, Bailly D, Maison C, Almouzni G. Mouse centric and pericentric satellite repeats form distinct functional heterochromatin. J Cell Biol 2004; 166:493–505.

36. Slijepcevic P. Telomeres and mechanisms of Robertsonian fusion. Chromosoma 1998;107:136–40.

37. Multani AS, Kacker RK, Pathak S. Are Robertsonian translocations rare in cancers? Cancer Genet Cytogenet 1997;93:179–80.

38. Cammarata M, Corsello G, Marino M, et al. Genetic factors of recurrent abortions. Acta Eur Fertil 1989;20: 367–70.

39. Fraccaro M. Chromosome abnormalities and gamete production in man. Differentiation 1983;23 Suppl:S40–3.

40. Frias S, Carnevale A, Zavaleta MJ, Molina B. Mitomycin C effect on Robertsonian translocations. Ann Genet 1988;31:162–6.

41. Adra CN, Boer PH, McBurney MW. Cloning and expression of the mouse pgk-1 gene and the nucleotide sequence of its promoter. Gene 1987;60:65–74.

42. Araki K, Araki M, Yamamura K. Targeted integration of DNA using mutant lox sites in embryonic stem cells. Nucleic Acids Res 1997;25:868–72.